Journal of Statistical Physics, Vol. 63, Nos. 5/6, 1991

On Some Transport Properties of Baker's Maps

Stephen Childress[1] **and Isaac Klapper**[1]

Received January 18, 1991

This paper considers the one-dimensional advection and diffusion of a passive scalar in the context of baker's maps of the unit interval. Our main interest is the thermal transport between two points held at fixed temperatures, when a deterministic sequence of maps of various scales are involved. Molecular diffusion occurs during the periods of rest between maps. We focus on the behavior of the transport in the limit of infinite Péclet number (or small molecular diffusion). Various asymptotic results are presented and compared with numerical calculations. Convergence to turbulent transport independent of molecular diffusion is observed as the number of scales is increased.

KEY WORDS: Transport; diffusion.

1. INTRODUCTION

The problem studied in this paper arose in work on fast dynamo action in some simple flows and Lagrangian maps.[1,2] In those studies the object was to determine the effect of iterated volume-preserving maps on the distribution and intensity of an embedded magnetic field. In the idealization adopted there, the magnetic field was equivalent to a field of material lines, so that the transport of the material vector field was calculated using a map. It was found that the determination of a positive growth rate of magnetic energy (dynamo action) introduced a nonstandard eigenvalue problem. The operator involved in calculating the new magnetic field, $TB(y)$ say, from an initial field $B(y)$ took the form

$$TB(y) = f(y)\, B(\tau(y)) \tag{1}$$

This paper is dedicated to Jerry Percus on the occasion of his 65th birthday.

[1] New York University, Courant Institute of Mathematical Sciences, New York, New York 10012.

0022-4715/91/0600-0897$06.50/0

where f and τ are functions, the former (as well as B) being generally complex, the latter being, in the case of a simple baker's (fold) map, the "tent" function, $\tau(y) = \min(2y, 1-2y)$ for the case where the domain of y is $[0, 1]$.

The iteration of (1) was seen to produce fields of increasing complexity in the sense that the oscillations of sign occur on scales which steadily reduce, and an "eigenfunction" of the problem must represent the completion in some sense of this process. The eigenvalue problem $TB = \lambda B$ is thus unusual, and must be understood in an appropriate weak topology. Modern methods of mutiresolution using wavelets would appear to be relevant to a formulation, but have not yet been implemented in the dynamo context. It therefore seems desirable to explore comparable problems in a simpler setting, where the advected field is scalar rather than vector.

The present discussion is thus devoted to the analogous problem of transport of a passive scalar field in simple baker's-type maps. For flows, the transport of a field $c(x, y, t)$ in two dimensions is governed by the dimensionless advection-diffusion equation

$$c_t + \mathbf{u} \cdot \nabla c - P^{-1} \nabla^2 c = 0 \tag{2}$$

where P is the Péclet number L^2/DT, with L and T being length and time scales and D a molecular diffusion coefficient; $\mathbf{u}$ is the velocity of the fluid, $\mathbf{u}(x, y, t) = (u, v)$. In the absence of diffusion, $D \equiv 0$ or $P \equiv \infty$, (2) states that the values of c are carried by the fluid, i.e., $c(x, y, t)$ is a material field. We shall study the transport of c in the limit in which diffusion is either zero or is small relative to advection. For definiteness we shall think of c as temperature and so adopt wherever helpful the terminology of heat conduction to describe the underlying transport phenomenon.

The basic problem of scalar transport is to compute average flux given a fixed mean gradient or boundary conditions such as fixed temperatures on two walls. Typically there is a scalar or matrix constant connecting heat flux and temperature gradient, in which case we speak of the computation of the effective diffusivity (or diffusivity matrix). If the flow responsible for the transport can be represented in some way by a map, then an underlying eigenvalue problem can be realized as follows: require the map to leave invariant the mean gradient while transporting the scalar at a fixed rate, and iterate indefinitely. The resulting field c would be the desired eigenfunction (or more properly a fixed point), if indeed convergence in a weak sense could be established. The map could then be taken as a crude approximation to the mixing imparted to the field by a complicated fluid motion, under steady-state conditions with fixed mean gradient.

To see how these ideas can arise in the simplest examples of baker's maps, consider the mapping of the unit square in $\mathbf{R}^2$ given by

$$(x, y) \to \begin{cases} (2x, y/2) & \text{if } 0 \leqslant x < 1/2 \\ (2x-1, (1+y)/2) & \text{if } 1/2 \leqslant x < 1 \end{cases} \tag{3}$$

(We will occasionally refer to the domain as a square, even though the fields considered in this paper will not depend upon x.) Imagine that the material in the square is initially at temperature $c(y)$, and diffusion is neglected, so that after one mapping the new temperature field is

$$c'(y) \equiv T_0 c(y) \equiv \begin{cases} c(2y) & \text{if } 0 \leqslant y < 1/2 \\ c(2y-1) & \text{if } 1/2 \leqslant y < 1 \end{cases} \tag{4}$$

Suppose, for example, that $c = G(y - 1/2)$, where the constant G is the initial temperature gradient. The average temperature over the square is then 0. We shall also refer to this as the initial *heat* contained in the square, assuming a unit specific heat for the material. In fact, the mean heat in the upper half of the square is initially $G/4$, while in the lower half it is $-G/4$. After the mapping given by Eq. (4), we see easily that the mean temperature is the same in top and bottom halves of the square, equal to 0. Thus we can say that the baker's map has "mixed" the material about the midline $y = 1/2$. In the process an amount of heat $G/8$ has been transported across this midline (since the heat content of 1/2 the square is 1/2 times the mean temperature there). The mixing has removed the mean temperature difference between the two halves.

In practice, real turbulent mixing involves similar processes where temperature gradients are locally reduced by mixing associated with fluid motions. Because of the complexity of the real motions, these events of mixing occur at various points and times, with the result that a fixed mean temperature gradient (imposed, e.g., by the boundary temperatures) is maintained, while heat is being transported down the gradient. The rate of heat transport thus realized is the basic unknown of the theory and depends on details of the flow field. Kerstein (refs. 3 and 4, and references given there) has carried out extensive studies of turbulent transport of a scalar based upon a baker's map description of the microscales. Kerstein's approach utilizes a probability distribution function for the position and size of the map. In the context of turbulent mixing the present remarks amount to a deterministic variant of Kerstein's class of models, with emphasis on the transport away from a boundary arising, for example, in turbulent Rayleigh–Bénard convection.

The renormalization procedure discussed in Section 8 is a simple example utilizing the one-dimensional setting of the problem. When the

velocity field itself is one dimensional in that it is a parallel flow, a large class of renormalizable models become accessible to rigorous treatment, as has been shown by Avellaneda and Majda.[5,6]

2. ADVECTION

When $D=0$ the process of renewal of the mean temperature gradient can be realized in a model based on Eq. (4) by extending the initial mean gradient to all y and introducing baker's maps for all points in the strip $0 \leqslant y < 1$. Let the first action of the maps be as described above; now mod 1 in y for the temperature *gradient*, but let the *second* mapping be carried out on intervals obtained by a vertical shift of 1/2. In particular, then, for our basic interval (interval 0 say, given by $0 \leqslant y < 1$), the second step will combine the top half with the bottom half of the interval above, say interval 1, while the lower half will combine with the top half of the interval below, say interval 1 (see Table I). With initial temperature $G(y-1/2)$, the mean heat in the top and bottom halves of interval 1 is $3G/4$. We focus on interval 0, with initial mean temperature $-G/4$ in the lower half, $+G/4$ in the upper half. After the first action of the map, these change to the identical "mixed" values 0; see above. (Note that interval n now has mean temperature n in both halves.) After the second application of the (shifted) map, however, we see that the temperature in interval 0 has a mean of $G/2$ in the upper half and $-G/2$ in the lower half, so an imbalance is restored, but to values different from the initial ones ($G/4$ and

Table I. Averages over 1/4 Intervals[a]

Interval	Initial value	Map 1	Map 2	Map 3	Map 4
1	11/8	5/4	2	3/2	2
	9/8	3/4	1	1/2	1
	7/8	5/4	1	32	1
	5/8	3/4	0	1/2	0
0	3/8	1/4	1	1/2	1
	1/8	−1/4	0	−1/2	0
	−1/8	1/4	0	1/2	0
	−3/8	−1/4	−1	−1/2	−1
−1	−5/8	−3/4	0	−1/2	0
	−7/8	−5/4	−1	−3/2	−1
	−9/8	−3/4	−1	−1/2	−1
	−11/8	−5/4	−2	−3/2	−2

[a] Two successive maps = S.

$-G/4$). Notice, however, that two further applications of the map lead to the same values of $G/2$ and $-G/2$ in interval 0, so that we are indeed maintaining the same mean temperature over halves of the intervals modulo 2 in applications of the map. The temperature distribution becomes a very complicated discontinuous function of y after a few iterations (we resolve it into quarter intervals in Table I), but if we regard dc/dy as a distribution, the mean gradient over an interval $[a, b]$ is just $\{c(b)-c(a)\}/|b-a|$, whose average value as a function of b is G.

Finally, we may compute the effective diffusivity in this model. We have already observed that the first application of the map led to a transport of $G/8$ units of heat across the midlines of each interval. The second application transfers $G/4$ in through the top boundary and out through the bottom boundary of each interval. Thereafter, the transfers are $G/4$ in both cases, leading to an equilibrium heat flux of $G/4$ units of heat per over the time associated with two applications of the map. If we define the effective diffusivity as

$$D_{\text{eff}} \equiv \text{flux}/G \cdot L^2/2\tau \tag{5}$$

where L is the physical dimension of a side of the basic interval and τ is the time required for one application of the map, we see that

$$D_{\text{eff}} = L^2/8\tau \tag{6}$$

The "shift" model illustrates how baker's maps can produce advective transport in its purest sense, namely a transport of heat independent of molecular diffusivity. Clearly if the temperature is resolved on a smaller scale than that shown in Table I, iteration leads to an equilibrium with more structure. We address the problem of determining the general equilibrium structure in the next section. Another basic question is the transport away from a rigid plane held at fixed temperature. The "shift" model cannot be extended up to such a plane. Finally, the scale of the baker's maps is an essential variable,[3,4], associated in a turbulent flow with the continuous distribution of eddy size. What happens if maps on many scales occur simultaneously? These and other matters can be addressed within the relatively simple class of deterministic models considered here.

3. FILTERED EQUILIBRIA WITHOUT DIFFUSION

We now refer to the period 2 map just outlined as the *shift map*. It is a paradigm of a mixing process based on a baker's map. We denote its operation on $c(y)$ by $Sc(y)$. We next show how to represent the

temperature field generated by S in terms of a new map on a single fixed interval.

We introduce a period 1 map which is closely associated with a full period (2) of the shift map. The *basic map* T is defined by

$$Tc(y) \equiv \begin{cases} c(2y) - 1/2 & \text{if } 0 \leqslant y < 1/2 \\ c(2y-1) + 1/2 & \text{if } 1/2 \leqslant y < 1 \end{cases} \tag{7}$$

Here we have included constants $\pm 1/2$ which restore the heat differential as part of the map, provided we now normalize the problem by setting $G = 1$ in the shift map. The basic map thus is of interest as a period 1 map. Indeed the idea is to replicate the transport by shifts as direct addition of heat, which can be effected on sufficiently small scales by molecular diffusion, although here such diffusion is absent.

To compare the maps S and T, we introduce the m-filter F_m, defined as the operator which maps $c(y)$ into the piecewise constant function on 2^m intervals of length 2^{-m}, in each of which $c(y)$ is replaced by its local average. Thus

$$F_m c(y) \equiv 2^m \int_{2^{-m}(k-1)}^{2^{-m}k} c(y)\, dy \quad \text{for} \quad 2^{-m}(k-1) \leqslant y < 2^{-m}k, \quad k = 1, 2, \ldots, 2^m \tag{8}$$

We denote the range of F_m by R_m. We now have the following elementary property:

Lemma 1. If T and F_m are defined by Eqs. (7) and (8), then $TF_m = F_{m+1}T$.

This result can be obtained by noting that $TF_m c(y)$ is in the range of F_{m+1}. Indeed, $(a_1, \ldots, a_m)^t$ is a column vector determining the constants involved in $F_m c(y)$. Thus, $TF_m c(y)$ is determined by the vector $(a_1 + 1/2, \ldots, a_m + 1/2, a_1 - 1/2, \ldots, a_m - 1/2)^t$, which is seen to also determine $F_{m+1} Tc(y)$.

We now may state the following result.

Theorem 1. Let $c_0(y) = -1/2$, $0 \leqslant y < 1/2$; $= 1/2$, $1/2 \leqslant y < 1$. Then $T^m c_0(y)$ is an element in the range of F_{m+1} which solves

$$F_{m+1} Tc(y) = F_{m+1} c(y), \qquad m = 0, 1, 2, \ldots \tag{9}$$

This is the only solution of Eq. (9) belonging to R_{m+1} and having zero average over the interval $[0, 1]$.

To prove this, we use induction. Note first that by direct calculation $F_1 Tc_0 = F_1 c_0$. Now assume that $F_m T^m c_0 = F_m T^{m-1} c_0$. Then, using the last equations together with Lemma 1 (twice), we have

$$F_{m+1} T^{m+1} c_0 = TF_m T^m c_0 = TF_m T^{m-1} c_0 = F_{m+1} T^m c_0 \tag{10}$$

which completes the induction step and establishes the solution. To prove uniqueness, let an element of R_{m+1} be denoted by $\mathbf{a} = (a_1, ..., a_{2^{m+1}})^t$. Then Eq. (9) can be represented as a matrix equation $A\mathbf{a} = \mathbf{f}$, where $\mathbf{f}$ is a column of 2^m 1's followed by 2^m -1's. The corresponding homogeneous equation has only solutions with all entries equal. The solution of (10) is therefore unique up to a multiple of such a vector, a suitable normalization being the condition in the theorem. This completes the proof.

Note that all $c(y)$ such that $T^m c(y) = T^m c_0(y)$ provide acceptable solutions, which form an equivalence class for each element of R_{m+1}.

The intuitive meaning of Theorem 1 is that iterates of c_0 under the basic map generate increasingly fine-scale, filtered "equilibrium temperatures" for the transport problem given by the basic map. We now show that these equilibria are also equilibria under the shift map, so that the basic map can replace the shift map as a generator of equilibria.

Theorem 2. $D \equiv F_{m+1} T^m c_0$ is also the $(m+1)$-filtered equilibrium for the period-2 shift map S.

We show this with a diagrammatic method. We let $A: B$ denote a square with $A(2y-1)$ in the top half, $B(2y)$ in the bottom half, and similarly $A: B: C: D$ will refer to quarter-squares from top to bottom. Starting with a square S, the basic property is that $S = S + 1/2: S - 1/2$ through an $(m+1)$-filter. Now after two steps the shift map produces $S+1: S: S: S-1$. But, again working through an $(m+1)$-filter, we see that

$$\begin{aligned} &S+1: S: S: S-1 \\ &\quad = (S+1/2: S-1/2) + 1/2: (S+1/2: S-1/2) - 1/2 \\ &\quad = (S+1/2: S-1/2) = S \end{aligned}$$

where we have simply applied the above property of S on intervals of arbitrary length.

Finally, we exhibit the spectral form of the basic map. We consider functions odd about $y = 1/2$, and therefore sine series of the form

$$c(y) = \sum_{n=1}^{\infty} a_n \sin(2\pi n y) \tag{11}$$

Let $T_c(y)$ have Fourier coefficients a_n^T. We compute

$$a_n^T = \begin{cases} -2/(\pi n) & \text{if } n \text{ is odd} \\ a_{n/2} & \text{if } n \text{ is even.} \end{cases} \tag{12}$$

Thus if c is an equilibrium, satisfying $Tc = c$, then we have a formal series of the form

$$c(y) = -2/\pi \sum_{p=1}^{\infty} \sum_{q=1}^{\infty} 1/(2p-1) \sin[2^q \pi (2p-1)\, y] \tag{13}$$

The antiderivative of this function converges absolutely.

Another representation for the same function comes from an expansion in a Haar basis. Let $H(y) = \operatorname{sgn}(y)$, $|y| \leqslant 1/2$; $= 0$, $|y| > 1/2$. Then it is clear from the iterations of the basic map that another representation of the equilibrium is

$$2c(y) = \sum_{k=1}^{\infty} \sum_{j=1}^{2^{k-1}} H(2^{k-1}[y - (2j-1)\, 2^{-k}]) \tag{14}$$

where filtering through F_m is truncation at $k = m$.

4. PIECEWISE LINEAR FUNCTIONS

We now consider a natural generalization of the basic map, which can be used in applications to advection of a magnetic field. Suppose, in particular, that we seek to construct results analogous to those of (7) within the class of *piecewise linear* functions. The motivation for this generalization comes from the magnetic problem of the unsteady fast kinematic dynamo. The SFS map can be reduced[1] to an operator G acting on a complex-valued function $b(y)$, defined on $[0, 1)$, given by

$$Gb(y) \equiv 2 \operatorname{sgn}(1/2 - y)\, e^{2\pi i \alpha (y - 1/2)} b(\tau(y)) \tag{15}$$

where

$$\tau(y) \equiv \min(2y, 2 - 2y) \tag{16}$$

is the "tent" function and α is the shear parameter. We now note that

$$\log e^{-i\pi/2} Gb(y) = \log b(\tau(y)) + \log 2 + 2\pi i \alpha (y - 1/2) + \operatorname{sgn}(y - 1/2)\, i\pi/2 \tag{17}$$

We thus now introduce a basic map on complex-valued functions $c(y) = \log b(y)$ defined by

$$Tc(y) \equiv \begin{cases} c(2y) + 2\pi i\alpha(y - 1/2) - i\pi/2 & \text{if } 0 \leqslant y < 1/2 \\ c(2-2y) + 2\pi i\alpha(y - 1/2) + i\pi/2 & \text{if } 1/2 \leqslant y < 1 \end{cases} \tag{18}$$

This new map differs from (7) in the fact that the tent map "turns over" the upper half of the square by a fold, by the complex-valued "temperature," and by the fact that the added function which is piecewise-linear in y instead of piecewise constant. The presence of the fold and complex values does not affect the essential argument in Section 3. When applied to piecewise-constant functions, the filtered equilibria may be computed as before by iteration from a simple initial condition. However, our previous arguments depended upon the piecewise-constant functions used, and we must modify our formulation.

The general form of our map is now

$$Tc(y) = c(\tau(y)) + 2a(y - 1/2) + b \operatorname{sgn}(y - 1/2) \equiv c(\tau(y)) + \gamma(y) \tag{19}$$

for arbitrary complex a, b. In order to proceed, we need a projection onto piecewise-constant fields at a given level of filtering. To see what has to be done, we consider a filter at a level $m = 1$. We would then expect, for a proper definition of projection, that $\gamma(y)$ as defined above would be an equilibrium. We have

$$T\gamma(y) = \begin{cases} -2ay + 2a + 2b & \text{if } 3/4 \leqslant y < 1 \\ -2ay + 2a & \text{if } 1/2 \leqslant y < 3/4 \\ 6ay - 2a & \text{if } 1/4 \leqslant y < 1/2 \\ 6ay - 2a - 2b & \text{if } 0 \leqslant y < 1/4 \end{cases} \tag{20}$$

We can see from the last equation how to define the appropriate filter to produce once again our initial function $\gamma(y)$. That is, we shall define a projection P_1 so that $P_1 T\gamma = \gamma$. Let F_m be as before the projection onto piecewise-constant fields, constant over intervals $I_m \equiv \{(0, 2^{-m}), (2^{-m}, 2^{1-m}), \ldots, (1 - 2^{-m}, 1)\}$, $I_0 = \{(0, 1)\}$. We allow F_m to operate on distributions provided the function is regular on I_m. Define $b^* = P_m b(y)$ as a function piecewise linear on I_m, whose derivative is piecewise constant on I_{m-1}, such that

$$F_{m-1}\, db^*/dy = F_{m-1}\, db/dy, \qquad F_m b^* = F_m b \tag{21}$$

In particular, $P_1 T\gamma$ must then have derivative $2a$ on I_0, and have average value $a/2 + b$ for $1/2 \leqslant y < 1$ and $-a/2 - b$ for $0 \leqslant y < 1/2$. This uniquely determines the piecewise linear function $P_1 T\gamma$ as γ.

With this definition it follows that $TP_m = P_{m+1}T$, and that $T^m\gamma$ then solves $P_{m+1}Tb(y) = P_{m+1}\gamma$, thus yielding a result paralleling Theorem 1.

For the magnetic problem our interest is in the growth rate p of the magnetic flux. We compute p from iterates of our basic map as follows: Introduce the *phase decrement*

$$q_m = Q_m/Q_{m-1}, \qquad Q_m \equiv \left| \int_0^1 e^{T^m\gamma}\, dy \right|, \qquad m = 1, 2,... \tag{22}$$

Then

$$p = \log 2 + \lim_{m \to \infty} \log q_m \tag{23}$$

Note that in the magnetic problem the constants a, b in γ are given by

$$a = 2\pi i\alpha, \qquad b = \pi i/2 \tag{24}$$

5. A BOUNDARY-VALUE PROBLEM WITH DIFFUSION

We now turn to a boundary-value problem, where the heat is applied through "walls," here the points 0 and 1, held at fixed temperature. We consider the case where the top wall, at $y = 1$, is held at temperature $1/2$ and the bottom wall, at $y = 0$, is held at temperature $-1/2$. (Recall the layer has a physical thickness L.) A baker's map is applied to the interval $(0, 1)$, the diffusion with coefficient D is allowed to act for a time τ. We can now represent the temperature $c_m(y)$ after the mth step (where one step is one map-diffusion sequence) in the form

$$c_m(y) = y - 1/2 + \sum_{n=1}^{\infty} a_{m,n} \sin(2\pi n y) \tag{25}$$

After one step, it is easy to show that the temperature field has the same structure with new Fourier coefficients

$$\begin{aligned} a_{m+1,n} &= (-1)^{n-1} D_n/\pi n, \qquad n \text{ odd} \\ &= [(-1)^{n-1}/\pi n + a_{m,n/2}]\, D_n, \qquad n \text{ even} \end{aligned} \tag{26}$$

where

$$D_n = \exp(-4\pi^2 n^2 D\tau/L^2) \tag{27}$$

From this we obtain the equilibrium temperature distribution at times $t = \tau -$:

$$\begin{aligned} c_{\text{eq}}(y) = y - 1/2 + \sum_{n=1}^{\infty} \sum_{m=1}^{\infty} (-1)^{n-1}/\pi n \sin(2^m \pi n y) \\ \times \exp[-4\pi^2 n^2 D\tau(4^m - 1)/3L^2] \end{aligned} \tag{28}$$

Evaluating $D\, dc_{eq}/dy$ at $y=1$, we obtain the effective diffusivity

$$D_{eff} = D + \sum_{n=1}^{\infty} \sum_{m=1}^{\infty} (-1)^{n-1}\, 2^m D \exp[-4\pi^2 n^2 D\tau(4^m - 1)/3L^2] \quad (29)$$

We rewrite the second term on the right, i.e., the advective contribution, in the form

$$D_{adv} = D^{1/2} L \sqrt{3}/2\pi \sqrt{\tau} \sum_{n=1}^{\infty} \sum_{m=1}^{\infty} \frac{(-1)^{n-1}}{n} 2^m z \exp[-z^2(4^m - 1)] \quad (30)$$

We now observe that the function

$$F(z) \equiv \sum_{m=1}^{\infty} 2^m z \exp[-(2^m z)^2] \quad (31)$$

has a limit as $z \to 0$. Indeed, we see that $F(1/2)$ exists and that

$$F(z/2) = z \exp(-z^2) + F(z) \quad (32)$$

It follows that the sequence $F(2^{-k})$ is monotone increasing and bounded above by $1 + F(1/2)$. Thus the limit exists. We compute $F(1/2) = 0.4045112$ and $F(0) = 1.2765484$ to seven places. Thus

$$D_{adv} = kL(D/\tau)^{1/2}, \qquad k \equiv F(0)\sqrt{3}/2\pi \log 2 = 0.2439178... \quad (33)$$

The heat flux through $y=1$ is actually a function of time between applications of the map,

$$D_{adv} = \sum_{n=1}^{\infty} \sum_{m=1}^{\infty} (-1)^{n-1}\, 2^m D \exp\{-4\pi^2 n^2 D[\tau(4^{m-1} - 1)/3 + t4^{m-1}]/L^2\} \quad (34)$$

where we measure time in units of τ. Computing the mean on $0 \leqslant t \leqslant \tau$, we find we again may make use of the function (31), and obtain

$$\langle D_{adv} \rangle = \tfrac{4}{3} D_{adv} \quad (35)$$

We evaluate the effective diffusivity divided by D in terms of the Péclet number P,

$$D_{eff}/D \equiv 1 + \langle D_{adv}/D \rangle \approx 1 + 4k/3P^{1/2}, \qquad P \equiv L^2/D\tau \gg 1 \quad (36)$$

Note that the square root dependence on P is typical of boundary layer enhancement of Bénard convection. In the cellular flows occurring there,

this enhancement is due to plume formation in boundary layers parallel to the direction of the mean temperature gradient. (For references pertaining to this problem and discussion of the exact Wiener–Hopf solution of the boundary-layer problem see ref. 7.) In the present example, the baker's map brings cool fluid to the top wall and warm fluid to the lower wall. In time τ a diffusive layer of thickness $(D\tau)^{1/2}$ is formed, and it is these layers, here *perpendicular* to the mean gradient, which are brought into the interior by subsequent maps and which produce the enhancement of heat flux given by the second term on the right of (36).

One further result can be obtained immediately from (34), and that is the mean-field value for D_{eff} obtained for *small* P. Integrating the flux and discarding the exponentially small terms, we obtain

$$\frac{D_{\text{eff}}}{D} \approx 1 + \frac{1}{4\pi^2} \sum_{n=1}^{\infty} \frac{(-1)^{n-1}}{n^2} P = 1 + \frac{P}{48}, \qquad P \ll 1 \tag{37}$$

6. A BOUNDARY-LAYER APPROXIMATION

We now show that a simple boundary-layer approximation gives a remarkably close approximation to (36) for small D. We shall assume that the heat flux on each boundary during the diffusion phase occurs into a thin, $O((D\tau)^{1/2})$ layer which may be studied as in a semi-infinite domain with a homogeneous condition at infinity. More precisely, we seek a function $c_b(y)$ defined in $y \geqslant 0$ satisfying

$$c_b(0) = 1, \qquad c_b(-\infty) = 0, \qquad H_\tau c_b(2y) = c_b(y) \tag{38}$$

where H_τ is the heat operator for the domain $y > 0$, mapping initial to final temperatures given the wall temperature of 1. This fixed-point problem is easily solved by working with the temperature gradient and introducing an initial gradient of the form $\exp(-cy^2)$; we obtain

$$c_b(y) = (2/\sqrt{\pi})\,\text{Erfc}(\eta), \qquad \eta = yL\sqrt{3}/[4(D\tau)^{1/2}] \tag{39}$$

Then

$$c(y) = -c_b(y)/2 + c_b(1-y)/2 + 1/2 \tag{40}$$

From (39) we obtain the layer diffusivity

$$D_b/D = 1 + 4k_b/3Pe^{1/2}, \qquad k_b \equiv (3/\pi)^{1/2}/4 = 0.2443031 \tag{41}$$

where we have used the fact that the flux at time τ stands here again in ratio 4/3 to the time mean of the heat flux. Comparing (41) with (33), we

see that the exact effective diffusivity is given by the boundary-layer approximation to an accuracy of about 0.0016. This is quite surprising, since the boundary-layer approximation neglects completely the contributions of layers of fluid which were heated and cooled at the walls and then mapped into the interior of the layer. These interior layers occur as "dipoles," however, and we can expect considerable cancellation as well as exponential decay of the residual temperature pulses. This is perhaps why the principale contribution is the local heat input from the wall.

This result invites exploitation in the more difficult environment of multiple-scale baker's maps. Let $T_0 \equiv T$ denote the map of the unit square, T_1 the map consisting of two maps of size 1/2 stacked one over the other, and so on. Let T_m be applied with period τ_m, where for convenience we assume that τ_0 is divisible by τ_m for each m, $\tau_0/\tau_m = p_m$. For a finite number of scales, $m = 1,..., M$, say, we may, in the limit of small D, adopt the boundary-layer approximation as before, since the boundary layer will be small compared to the smallest map occurring in the sequence. Within the boundary layer, moreover, the effect of the maps T_m is the same for all m. Thus, if H_τ stand for diffusion according to the heat equation for time τ, the operations over one cycle are equivalent to

$$H_{\tau_M} T^{\mu_{p_M}} H_{\tau_M} T^{\mu_{p_M}-1} \cdots H_{\tau_M} T^{\mu_1} \tag{42}$$

where the positive integers μ_i depend upon the p_m. If we synchronize all scales to start simultaneously, then $\mu_1 = M$. For example, if $M = 2$ and $\tau_1 = \tau_0/2$, we obtain the one cycle of maps $H_{\tau_0/2} T H_{\tau_0/2} T^2$.

The problem of main interest is, however, when the smallest scale is zero, so that, for any $D > 0$, some maps operate in a regime where the boundary-layer approximation is not valid and molecular diffusion is important on the corresponding time and length scales. We turn now to the numerical calculation of transport by maps on more than one scale.

7. NUMERICAL SOLUTIONS WITH MULTIPLE SCALES

Our plan is to utilize a binary partition of the unit interval for numerical solution of the heat equation using a fast Fourier transform, embedded in a binary partition into maps. We divide the interval into $N \equiv 2^J$ intervals of length $2^{-J}L$, with 2^K of these intervals used to resolve a map. There are then 2^M maps, where $M = J - K$. Here $J > K \geqslant 0$. If the time interval between maps (i.e., the period) is τ, we need to resolve down well below $(D\tau)^{1/2}$. Thus, in practice we want $2J \gg \log L^2/D\tau/\log 2 \approx M$ in order to study cases where the boundary-layer approximation is not possible.

The first problem to consider is the periodic application of 2^M maps with period τ. Because of the symmetry of the boundary-value problem, the solution can be obtained by rescaling the case $M=0$ studied in Section 5. For example, (36) again applies with P replaced by $4^{-m}P$. In Fig. 1, curves 1 and 2 compare the boundary-layer approximation to $\log(2D_{\text{eff}}/D)$ vs. $\log P$ with the exact result given in Section 5 as computed by the program using fast Fourier transforms. The asymptote to the left matches well with the mean field approximation for small P given by (37).

Curve 3 and 4 of Fig. 1 are for the following multiple-scale cases: For curve 3, two maps on intervals of length $L/2$ are applied with period $\tau/2$, while a single map on scale L is applied with period τ. For curve 4, maps on seven scales, i.e., on equal intervals of length 2^{-M} for $M=0, 1,..., 6$, are applied simultaneously with period τ. The cases enhance transport, but again have a $P^{1/2}$ behavior at large P. For both 3 and 4, the slope at the smaller values of P is larger, indicating enhanced transport associated with the smaller scales, but the asymptotic behavior for large P is essentially the same. This can be understood from the boundary-layer structure. Near the wall dc_b/dy is a Gaussian with coefficient $3P/16$ at the termination of one cycle; cf. (39). For the 2, $2+1$ case this coefficient changes to $63P/160$. Computing integrated fluxes over the two intervals period $\tau/2$, we find that k_b in (41) is increased by a factor 1.67 approximately. This yields an

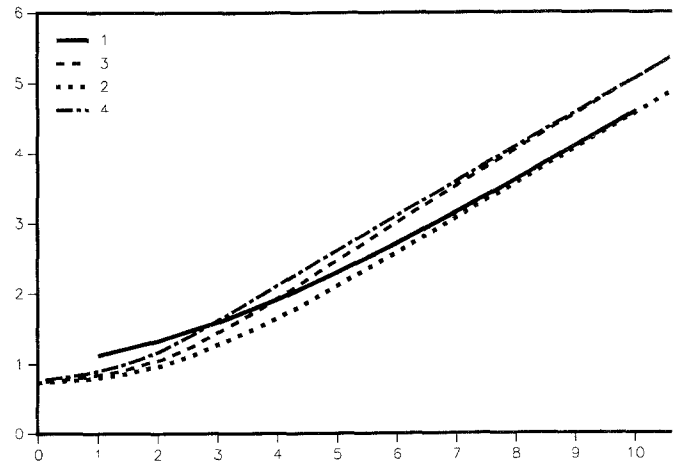

Fig. 1. $\log(2D_{\text{eff}}/D)$ vs. $\log P$. Curve 1: boundary-layer approximation (36) for a single map. Curve 2: Numerical computation for a single map. Note that for 2^M equal maps, curves 1 and 2 are shifted to the right an amount $2M \log 2$. Curve 3: 2 maps at $t=0+$, $2+1$ maps at $\tau/2$, 2 maps at τ, and so on. (Here $2+1$ means two maps on the scale $L/2$ are followed by one map on scale L.) Curve 4: $1+2+4+8+16+32+65$ maps with period τ. In all cases $N=1024$.

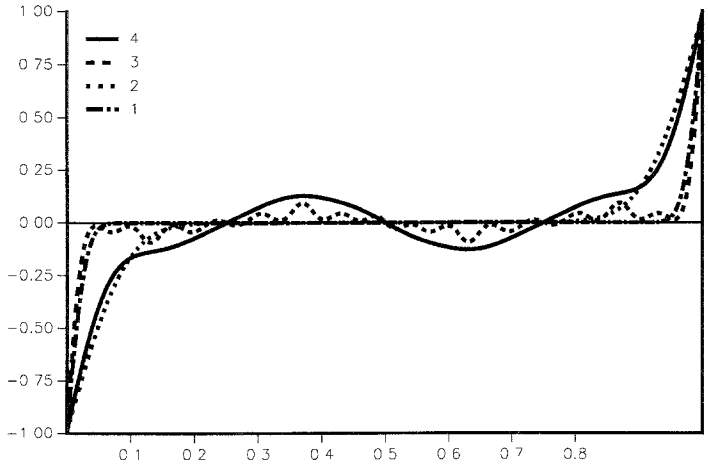

Fig. 2. $c(y)$ vs. y after ten iterations. Curve 1: $1+2+4+8+16+32+64$ maps with period τ, $P=400\pi^2$. Curve 2: Same as curve 1, $P=40\pi^2$. Curve 3: 2 maps at $t=0+$, $2+1$ maps at $\tau/2$ (cf. caption for curve 3 of Fig. 1), $P=400\pi^2$. Curve 4: Same as curve 3, $P=40\pi^2$.

increase in the ordinate of Fig. 1 of 0.51, compared with the computed value of 0.49. For curve 4 the large compression from the seven maps puts the enhancement of k_b according to the boundary-layer approximation very close to its maximum $\sqrt{3}$, increasing the ordinate in the figure by 0.54. The computed value of is about 0.48. Curve 4 suggests that the $\sqrt{P}$ asymptote is realized once log P exceeds about 8, corresponding to a boundary layer thickness of about 1/27. This is reasonable since only a few of the seven scales are needed to attain the limiting form, and a thickness of 1/27 allows maps down to size 2^{-4} to easily contain the boundary layer.

We now turn to cases which are attractive for renormalization of the effective transport, and introduce the enhanced transport associated with the heat transfer of the basic map on arbitrarily small diffusive scales. The approach will be an obvious application of renormalization principles to the large-P theory. If we take the Péclet number as the transport parameter, then (36) may be written

$$P_{\text{eff}} = F(P) \equiv P/(1+4k\sqrt{P}/3) \tag{43}$$

We consider maps on equal intervals of length $L_j = 2^{-M_j}L$ with period $\tau_j = 2^{-\lambda_j M_j}$, where M_j is an integer and λ is a real number. Then in the asymptotic regime $P_j = \gamma_j^{-1}F(\gamma_j P)$ is the effective Péclet number, where $\gamma_j = L_j^2\tau_{j+1}/L_{j+1}^2\tau_j$. If $L_1 \ll L_2 \ll \cdots \ll L_r \ll L_{r+1} \equiv L$ denotes some finite set of nested lengths, then if the boundary layer for maps of size L_{j+1} contains many maps on the smaller scale L_j, we can represent the effect of the

smaller maps in terms of an effective P, relative to the scale L_{j+1}. The condition that this is a reasonable assumption is that $L_j/L_{j+1} \ll 4/(3P_j)^{1/2}$. In this case we can compute P_{r+1}/P_0 (where $P_0 \equiv P$) by iteration,

$$P_{j+1} = \gamma_{j+1}^{-1} F(\gamma_{j+1} P_j), \qquad j = 0, 1, \ldots, r \tag{44}$$

We show in Fig. 3 the case $r = 1$ with maps of size $L/8$ and period $\tau/8$ embedded in the single map. The condition for validity of the renormalization requires both that P be large and that the above condition on the L_j be satisfied. In the present case, at $P = 600$ the boundary layer contains about two small cells, certainly the limit of validity. The break in curve 2 of Fig. 3 toward the asymptotic slope of 1/2 is consistent with this estimate. When $\log P$ is between 4 and 9 approximately, the $P^{3/4}$ dependence obtained asymptotically is roughly followed. The fact that the asymptotic formula overestimates the transport is presumably a result of the fact that this "window" does not extend to high enough P; cf. Fig. 1.

We now generalize the asymptotic expression to an infinite number of scales, through a cascade to intervals of arbitrarily small size. We use

$$P_{j+1}^2 \approx 3P_j/(16k^2\gamma_{j+1}) \tag{45}$$

Let $M_i = iM$, $\lambda_j = \lambda$, where λ is a real constant and 2^{-M} is the scale reduction in one step of the cascade. Iteration through $r+1$ steps then yields

$$\log P_{r+1} = \log\left[\frac{3}{16k^2 2^{(\lambda-2)M}}\right]\left(\frac{1-1}{2^{r+1}}\right) \tag{46}$$

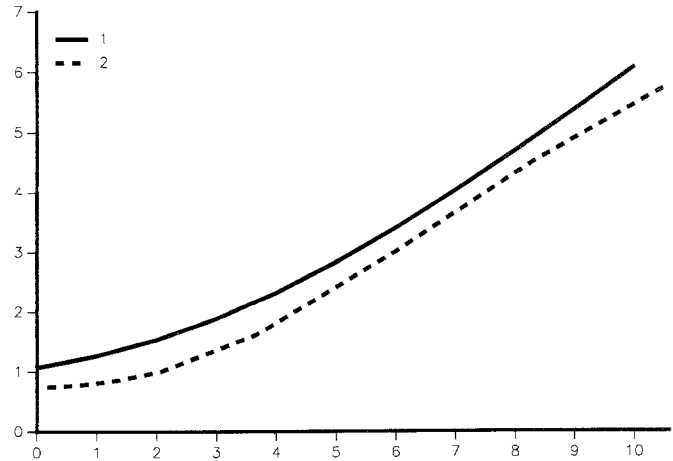

Fig. 3. $\log(2D_{\text{eff}}/D)$ vs. $\log P$. Renormalization on one microscale, $r = 1$, $L_1 = L/8$, $\tau_1 = \tau/8$. Curve 1: Asymptotic approximation for large P, given by $\log(2P/P_2)$, where $P_2 = F(P_1)$, $P_1 = 8f(P/8)$. Curve 2: Computations for the same sequence of maps.

In the limit of large r we find

$$1/P_{\text{eff}} = 16k^2 2^{(\lambda-2)M}/3 \tag{47}$$

We thus obtain an effective diffusivity which is independent of molecular diffusivity, but without the use of the shift. The enhanced transport here arises from the fact that there are always scales sufficiently small to act like the basic map, in that the local diffusivity is of order 1. This allows heat to be transported away from a wall, where it is further mixed up the sequence of maps of ever larger scale. We note that if $M=1$ in (47) and λ takes on the Kolmogorov value of 2/3, we obtain $D_{\text{eff}}\tau/L^2 = 0.126$, which is almost exactly the value for the shift map; cf. (6).

8. CONCLUDING SUMMARY

Although simple baker's maps are discontinuous transformations in both space and time, they can mimic certain features of transport of both scalar and vector fields by continuous fluid flows at small molecular diffusivity. In effect, a map provides a simple mixing process in the manner of a turbulent "eddy." For the case of heat conduction through a fluid layer, our kinematic study shows that baker's maps can simulate turbulent transport of a kind that depends strongly on molecular diffusion at small scales. On the other hand, away from a rigid boundary a simple shift map can achieve the same result in an ideal fluid. There are analogous results for the transport of a nearly material vector field, but in the case of fast dynamo theory there is as yet no technique comparable to the boundary-layer theory used here. In that problem the magnetic field is distributed intermittently throughout the fluid, but it may be that these patches of field can be treated individually as free boundary layers.

The large-P theory developed here parallels that of certain simple steady flow fields,[8,9] although the source of the $P^{1/2}$ behavior of D_{eff}/D for large P is different for maps and fluid eddies. For closed eddies in a thermal gradient the fluid which is warmed or cooled at the eddy boundary is swept into a plume extended in the direction of the mean gradient, and it is here that the enhanced mixing occurs. For a map the fluid is swept (at least in part) directly into the interior. For extensions of the theory these differences may be minor, however. In particular, the results given in refs. 8 and 9 would appear to allow an analogous renormalization argument over fluid eddies on many scales.

REFERENCES

1. B. Bayly and S. Childress, *Geophys. Astrophys. Fluid Dynam.* **44**:211 (1988).
2. B. Bayly and S. Childress, *Geophys. Astrophys. Fluid Dynam.* **49**:23 (1989).
3. Alan R. Kerstein, *J. Fluid Mech.* **216**:411 (1990).
4. Alan R. Kerstein, Preprint (1990).
5. Marco Avellaneda and Andrew J. Majda, *Commun. Math. Phys.* **131**:381 (1990).
6. Marco Avellaneda and Andrew J. Majda, CNRS preprint (1990).
7. A. M. Soward, *J. Fluid Mech.* **180**:267 (1987).
8. S. Childress and A. M. Soward, *J. Fluid Mech.* **205**:99 (1989).
9. A. M. Soward and S. Childress, *Trans. R. Soc. Lond. A* **331**:649 (1990).